Novel Design of AlGaInAs–InP Lasers Operating at 1.3 μm

R. F. Kazarinov and G. L. Belenky

Abstract— **A novel design of AlGaInAs–InP lasers operating at 1.3 μm is proposed. A distinctive attribute of the proposed design is that the AlInGaAs active region is surrounded by an AlInAs electron stopper layer on the p-side and an InP hole stopper layer on the n-side. The stopper layers do not impede the carrier injection into the active region and at the same time reduce the thermionic emission of carriers out of the active region. Utilization of stopper layers allows one to increase the value of internal quantum efficiency and to select the waveguide material corresponding to the optimum optical confinement factor value.**

I. Introduction

SINCE density of states of a two-dimensional electron gas near the energy gap is larger than that of a bulk material, single quantum-well (SQW) lasers have a higher material gain than bulk active region lasers [1]. However, the optical occupation factor of a quantum well is very small and so is the modal gain. In order to achieve high quantum efficiency and low threshold current density, SQW lasers should have large cavity length and small free carrier absorption in the waveguide layer. Quantum-well lasers have been successfully demonstrated for a GaAlAs–GaAs material system [2], [3] and have become an industrial reality. GaAlAs–GaAs lasers with one or two 40-Å–100-Å-wide quantum wells have been adopted for most practical applications [4]. In the latter material system the discontinuities of conduction bands are larger than those of valence bands. Therefore quantization of both electron and hole states in quantum wells is possible in spite of a small ratio of electron and hole effective masses. Large differences in energy gaps and refractive indices between GaAs and AlAs allow both the electronic properties mentioned above and a high value of the optical occupation factor.

It is difficult to obtain similar conditions for an InGaAsP–InP system used for communication lasers due to a small conduction band discontinuity between InP and the active region material [5]. In addition, a low potential barrier for electrons between the active and cladding regions also results in thermionic emission of electrons out of the active layer [6], [7]. In order to overcome this problem, a high doping level of cladding layers is necessary, producing high optical absorption of the lasing mode. An adequate modal gain for this type of laser has been achieved by stacking quantum wells and separating them with potential barriers, thus forming a multiquantum-well (MQW) structure. However, due to the noted problems and Auger recombination characterizing narrow-gap materials, InGaAsP–InP-based lasers demonstrate strong temperature dependence on threshold currents and external quantum efficiency [8].

An improved temperature performance of 1.3-μm strained quantum-well lasers was reported in [9], where AlInGaAs–InP material system was used to increase the electron confinement energy. The result was attainable due to a better fit of the discontinuities of the conduction and valence bands of AlInAs and GaInAs (matching those of InP). The characteristic temperature of threshold current (T_0) reported in [9] was 80 K.

In this paper, we propose and analyze a novel laser design which utilizes the electron affinity difference between AlInAs and InP to improve the confinement of electrons in the active region and optical confinement of the lasing mode in the waveguide. According to the results of modeling, the laser structure proposed here has significantly higher quantum efficiency than the devices described in [9] and is characterized by $T_0 = 100$ K.

II. Device Structure and Modeling

The device structure is presented in Fig. 1. All values of energy gaps E_g and refractive indices ν of the materials are shown in Table I. The structure consists of n- and p-AlInAs cladding layers followed by n- and p-AlInGaAs (I) waveguide layers. In the structure the active layer is surrounded by an AlInAs electron stopper layer on the p-side and an InP hole stopper on the n-side. InP and AlInAs lattice matched to InP have almost equal E_g values, but the electron affinity of InP is 0.35 eV larger than that of AlInAs. The existence of stopper layers does not impede the injection of carriers into the active region and at the same time drastically reduces the thermionic emission of carriers out of the active layer. Therefore, the selection of E_g for waveguide materials is now limited not by the value of recombination current in the waveguide region but by the value of the interband optical absorption of laser emission. When $\alpha \sim 1$ cm^{-1}, E_g of the waveguide materials for lasing wavelength 1.3 μm can be selected as low as 1.02 [10]. This option obviously allows significant improvement in the optical occupation factor of the active layer. The active region of the structure includes three undoped AlInGaAs quantum wells and four AlInGaAs (II) barriers. Fig. 2 shows the energy diagram of a 40-Å-wide quantum well. The potential barrier for electrons in this well is $\Delta E_c = 0.3$ eV and for holes $\Delta E_v = 0.12$ eV. As shown in Fig. 2 electrons have only one bound state with energy 0.138 eV which corresponds to zero kinetic energy of a two-dimensional motion in the quantum-well plane. Two

Manuscript received July 22, 1994; revised October 12, 1994.
The authors are with AT&T Bell Laboratories, Murray Hill, NJ 07974 USA.
IEEE Log Number 9408599.

0018–9197/95$04.00 © 1995 IEEE

Doping	Layer	Material	Thickness
$5 \times 10^{17} cm^{-3}$	cladding layer	p-AlInAs	
$2 \times 10^{17} cm^{-3}$	waveguide	p-AlInGaAs (I)	1200Å
$2 \times 10^{17} cm^{-3}$	electron stopper	p-AlInAs	100Å
$1 \times 10^{17} cm^{-3}$	barrier	p-AlInGaAs (II)	100Å
undoped	**active**	**AlInGaAs**	40Å
$1 \times 10^{17} cm^{-3}$	barrier	p-AlInGaAs (II)	100Å
undoped	**active**	**AlInGaAs**	40Å
$1 \times 10^{17} cm^{-3}$	barrier	n-AlInGaAs (II)	100Å
undoped	**active**	**AlInGaAs**	40Å
$1 \times 10^{17} cm^{-3}$	barrier	n-AlInGaAs (II)	100Å
$1 \times 10^{17} cm^{-3}$	hole stopper	n-InP	80Å
$1 \times 10^{17} cm^{-3}$	waveguide	n-AlInGaAs (I)	1200Å
$1 \times 10^{18} cm^{-3}$	cladding layer	n-AlInAs	
$2 \times 10^{17} cm^{-3}$	substrate	n-InP	

Fig. 1. Schematic cross section of a laser structure. The parameters of the materials are shown in Table I.

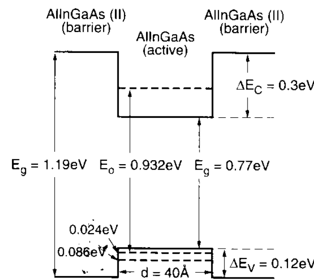

Fig. 2. Energy diagram of a 40-Å-wide quantum well. Energies of electron and hole ground states are counted from the bottom of the corresponding band.

TABLE I
ENERGY GAPS E_g AND REFRACTIVE INDICES ν OF MATERIALS

Materials	E_g (eV)	v
AlInAs	1.47	3.16
AlInGaAs	0.770	3.55
AlInGaAs (I)	1.02	3.455
AlInGaAs (II)	1.190	3.322
InP	1.35	3.21

hole bound states with energies 0.024 eV and 0.086 eV are separated by an energy distance exceeding 2 kT at $T = 300$ K. In calculating the energetical structure in Fig. 2 we used the values of effective electron masses of 0.045 m_0 and 0.067 m_0 for the materials of the wells and the barriers respectively, where m_0 is a free electron mass. The effective masses of holes used were 10 times larger than electron masses.

Fig. 3 shows the sheet gain $G = d^* g$ (where d is a quantum-well width and g is a quantum-well material gain) versus sheet carrier density N. The dependence $G(N)$ is calculated in the framework of model [11]. The data in Fig. 3 corresponds to a single quantum well at 1% compressive strain.

The modal gain g_m is related to G by the following equation:

$$g_m = \frac{G}{W} \quad (1)$$

where the effective optical mode width W is defined as

$$W = \frac{\int_{-\infty}^{+\infty} E^2(x)\,dx}{E^2(0)} \quad (2)$$

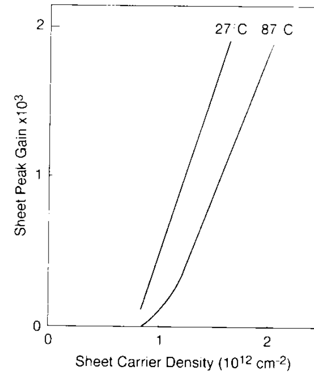

Fig. 3. Sheet gain versus sheet carrier densities calculated for a 1.3-μm laser in the framework of model [11].

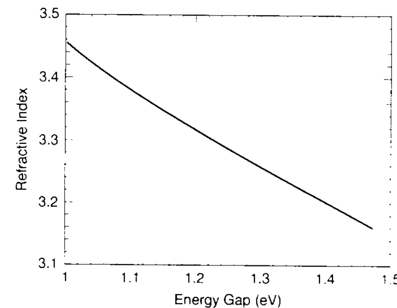

Fig. 4. Dependence of refractive indices on the energy gap of AlInGaAs materials lattice-matched to InP calculated in the framework of a three-parameter model [12].

with $E(x)$ the amplitude of the generated light wave with the maximum value at $x = 0$ and x is the coordinate along the growth direction. The value of W is determined by the difference between the refractive indices of the cladding and waveguide layers as well as by the width of the waveguide layer. It is clear (see (1)) that a reduction of W value leads to an increase of the model gain g_m.

Fig. 4 shows the dependence of refractive indices of the energy gap of AlInGaAs materials lattice matched to InP. The dependence $v(E_g)$ was calculated in the framework of a three parameter model [12] using the experimental values of refractive indices for AlAs [12] and InGaAs [13]. The results of the experimental measurements of refractive indices for AlGaInAs materials were recently published in [14]. The calculated values of refractive indices shown in Fig. 4 shift relative to the experimental data by −(0.05–0.07). This shift does not affect the results of our calculations since they depend only on the difference between the indices of the waveguide and the cladding layers, but not on their absolute values.

The value of W calculated for the structure shown in Fig. 4 is $W = 3.6\ 10^{-5}$ cm. It should be emphasized that using a conventional approach and selecting the same waveguide and barrier material the optimal value of W would have been $W = 5\ 10^{-5}$ cm. The threshold sheet carrier concentration N_{th} can be calculated for a given total loss α_{total} using dependence of $G(N)$ from Fig. 3 and the value of W.

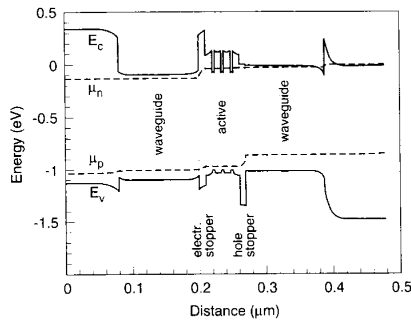

Fig. 5. Band diagram of a laser structure under bias conditions.

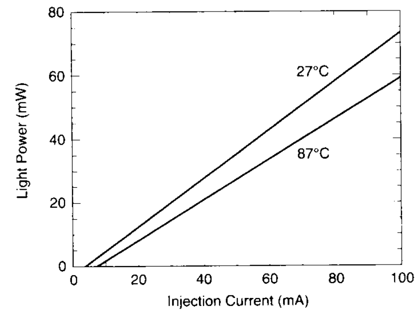

Fig. 6. Calculated light power versus injection current for a laser with a 500-μm cavity length and mesa width of 3 μm.

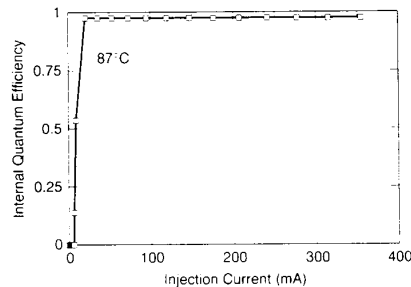

Fig. 7. Calculated internal efficiency versus injection current for a laser with a 500-μm cavity length and mesa width of 3 μm.

Fig. 5 shows the band diagram of the laser under bias conditions calculated by Padre program [6]. In the calculations we used the values of $N_{\rm th}$ = 1.04 10^{12} cm^{-2} at 27°C and $N_{\rm th}$ = 1.35 10^{12} cm^{-2} at 87°C which correspond to total optical losses of 30.87 cm^{-1} and 32.37 cm^{-1}. The value of $\alpha_{\rm total}$ includes losses at the mirrors and free carrier absorption in a cavity 500 μm long. We used for the coefficient of free carrier absorption α_i = 6 cm^{-1} and 7.5 cm^{-1} at 27°C and 87°C, respectively [9], [15]. The values of the two-dimensional Auger recombination coefficients at 27°C and 87°C were selected according to [16] C_{2D} = 0.72 10^{-16} cm^4 s^{-1} and C_{2D} = 0.86 10^{-16} cm^4 s^{-1}. The two-dimensional radiative recombination coefficient in a quantum well was calculated from a three-dimensional value 0.8878 10^{-10} cm^3 s^{-1} taking into account the well width of 40 Å. The mobility values of electrons and holes in the waveguide and cladding layers were selected to be identical to those in GaAs. Since the barrier thickness in the structure is about 100 Å the probability of carrier tunneling is negligible and transport of carriers through the active region is described by thermionic process.

The bandgap of a quantum well shown in Fig. 5 was 0.9321 eV, which corresponds to the difference in the energies between the electron and hole ground states in a two-dimensional quantum well (see Fig. 2). One can see in Fig. 5 that the difference between the electron (μ_n) and hole (μ_p) quasi-Fermi levels is smaller in the waveguide materials than in the active region. It means that the total recombination rate in the waveguide layers is reduced due to the presence of the electron and hole stopper layers in the structure. We would like to emphasize that the potential drops at the interfaces between the cladding and waveguide layers can be significantly reduced by replacing the abrupt junctions shown in Fig. 5 by graded structures.

Fig. 6 shows calculated light power versus injection current for lasers with a 500-μm cavity length and mesa width of 3 μm at 27°C and 87°C. The corresponding threshold currents are 4 mA and 7.3 mA and threshold current densities are 264 A/cm^2 and 481.8 A/cm^2. The T_0 value is 100 K. The slope efficiencies are $\eta_{\rm ex} = 0.8$ at room temperature and $\eta_{\rm ex} = 0.659$ at 87°C. It is well known that $\eta_{\rm ex}$ is determined by the product of internal quantum efficiency $\eta_{\rm int}$ and the ratio of mirror loss to the total loss. One can see from Fig. 7 that $\eta_{\rm int}$ makes no significant contribution to the external efficiency of the device even at 87°C. The laser structure chosen in this paper is not the only one whose characteristics can be improved by utilization of electron or hole stopper layers. For example, a hole stopper layer can improve the performance of GaAs-based lasers. Utilization of an InAlAs electron stopper layer in a InGaAsP laser structure allows to avoid electron leakage into the p-cladding layer. In this case, InP can be selected as a material for cladding layers in Fig. 1 while the barriers and the active quantum wells can be made of InGaAsP epilayers. The results of modeling for the latter structure will be published separately.

III. Conclusion

We propose a novel design of AlGaInAs–InP lasers operating at 1.3 μm. A distinctive attribute of the proposed design is that the AlInGaAs active region is surrounded by an AlInAs electron stopper layer on the p-side and an InP hole stopper on the n-side. The stopper layers do not impede the carrier injection into the active region and at the same time reduce the thermionic emission of carriers out of the active region. Utilization of stopper layers allows an increase in the value of internal quantum efficiency and the selection of a waveguide material corresponding to the optimum optical confinement factor value. The use of stopper layers in laser structures is generally not limited by the material system analyzed in the present paper. For example, the incorporation of an electron stopper layer can improve the characteristics of InGaAsP-based laser structures and a GaInAs–GaAs-hole stopper layer will help to reduce the hole leakage from the active region of GaAs-based lasers.

REFERENCES

[1] R. Dingle and C. H. Henry, "Quantum effects in heterostructure lasers," U.S. Patent 3 982 207, 1976.

[2] W. T. Tsang, C. Weisbuch, R. C. Miller, and R. Dingle, "Current injection GaAs-AlInAs multiquantum well heterostructure lasers prepared by molecular beam epitaxy," *Appl. Phys. Lett.*, vol. 35, p. 673, 1979.

[3] W. T. Tsang, "Extremely low threshold (AlGa)As modified multiquantum well heterostructure lasers grown by molecular-beam epitaxy," *Appl. Phys. Lett.*, vol. 39, pp. 786–788, 1981.

[4] P. S. Zory, Jr. (Ed.), *Quantum Well Lasers*. Orlando, FL: Academic, 1993.

[5] M. S. Hybertsen, "Band offset transitivity at the InGaAs/InAlAs/InP (001) heterointerfaces," *Appl. Phys. Lett.*, vol. 58, no. 16, p. 1759, 1991.

[6] R. F. Kazarinov and H. R. Pinto, "Carrier-transport in laser heterostructure," *IEEE J. Quantum Electron.*, vol. 30, pp. 49–54, 1994.

[7] G. L. Belenky, R. F. Kazarinov, J. Lopata, S. Luryi, T. Tanbun-Ek, and P. A. Garbinski, "Direct measurement of the carrier leakage out of the active region in InGaAsP/InP laser heterostructures," *IEEE Trans. Electron Devices*, to be published.

[8] P. J. A. Thijs *et al.*, "High output power (380 mW) low threshold (1.3 mA), low linewidth enhancement factor $\lambda = 1.3$ μm strained quantum well lasers," in *Proc. 17th European Conf. Opt. Commun.*, Paris, Sept. 9–12, 1991, pp. 48–51.

[9] C. E. Zah, R. Bhat, B. Pathak, F. Favire, M. C. Wang, W. Lin, N. C. Andreadakis, D. M. Hwang, M. A. Koza, T. P. Lee, Z. Wang, D. Darby, D. Flanders, and J. F. Hsieh, "High-performance uncooled 1.3-μm $Al_xGa_yIn_{1-x-y}As$/InP strained-layer quantum-well lasers for fiber-in- the-loop applications," in *OFC 94 Tech. Dig.*, vol. 4, p. 204.

[10] C. H. Henry, R. A. Logan, H. Temkin, and F. R. Merrit, "Absorption, emission and gain spectra of 1.3 μm InGaAsP quaternary lasers," *IEEE J. Quantum. Electron.*, vol. 19, pp. 941–946, 1983.

[11] D. Gershoni, C. H. Henry, and G. A. Baraff, "Calculating the optical properties of multidimensional heterostructures," *IEEE J. Quantum Electron.*, vol. 29, pp. 2433–2451, 1993.

[12] M. A. Afromowitz, "Refractive index of $Ga_{1-x}Al_xAs$," *Solid State Commun.*, vol. 15, pp. 59–63, 1974.

[13] Toru Takaqi, "Refractive index of $Ga_{1-x}In_xA_s$ prepared by vapor-phase epitaxy," *Japan J. Appl. Phys.*, vol. 17, pp. 1813–1817, 1978.

[14] M. J. Mondry, D. I. Babic, J. E. Bowers, and L. A. Coldren, "Refractive indexes of (Al,Ga,In)As epilayers on InP for optoelectronic applications," *IEEE Photonics Tech. Lett.*, vol. 4, pp. 627–630, 1994.

[15] C. H. Henry, R. A. Logan, F. R. Merritt, and J. P. Luongo, "The effect of intervalence band absorption on the thermal behavior of InGaAsP lasers," *IEEE J. Quantum Electron.*, vol. 19, pp. 947–952, 1983.

[16] G. Fuchs, C. Schiedel, A. Hangleiter, V. Harle, and F. Schoolz, "Auger recombination in strained and unstrained InGaAs/InGaAsP multiple quantum-well lasers," *Appl. Phys. Lett.*, vol. 62, pp. 396–398, 1993.

R. F. Kazarinov, photograph and biography not available at the time of publication.

G. L. Belenky, photograph and biography not available at the time of publication.